Control modulation instability in photorefractive crystals by the intensity ratio of background to signal fields

Chien-Chung Jeng,[1,*] **Yonan Su,**[2] **Ray-Ching Hong,**[2] **and Ray-Kuang Lee**[2]

[1]*Department of Physics, National Chung-Hsing University, Taichung 402, Taiwan*
[2]*Institute of Photonics Technologies, National Tsing-Hua University, Hsinchu 300, Taiwan*
∗ccjeng@phys.nchu.edu.tw

Abstract: By experimental measurements and theoretical analyses, we demonstrate the control of modulation instability in photorefractive crystals though the intensity ratio of coherent background to signal fields. Appearance, suppression, and disappearance of modulated stripes are observed in a series of spontaneous optical pattern formations, as the intensity of input coherent beam increases. Theoretical curves based on the band transport model give good agreement to experimental data, both for different bias voltages and different intensity ratios.

OCIS codes: (190.0190) Nonlinear optics; (190.3270) Kerr effect; (190.5330) Photorefractive optics.

References and links

1. T. Shinbrot and F. J. Muzzio,"Noise to order," Nature **410**, 251 (2001).
2. V. I. Bespalov and V. I. Talanov, "Filamentary structure of light beams in nonlinear liquids," J. Exper. Theor. Phys. Lett. **3**, 307 (1966).
3. V. I. Karpman, "Self-modulation of nonlinear plane waves in dispersive media," J. Exper. Theor. Phys. Lett. **6**, 277 (1967).
4. T. B. Benjamin and J. E. Feir, "The disintegration of wave trains on deep water," J. Fluid Mech. **27**, 417 (1967).
5. A. Hasegawa, *Plasma Instabilities and Nonlinear Effects,* (Springer-Verlag 1975).
6. G. P. Agrawal, *Nonlinear Fiber Optics*, 3rd ed. (Academic, 2001).
7. M. I. Carvalho, S. R. Singh, and D. N. Christodoulides, "Modulational instability of quasi-plane-wave optical beams biased in photorefractive crystals," Opt. Commun. **126**, 167 (1996).
8. C. C. Jeng, Y. Y. Lin, R. C. Hong, and R.-K. Lee, "Optical Pattern Transitions from Modulation to Transverse Instabilities in Photorefractive Crystals," Phys. Rev. Lett. **102**, 153905(2009).
9. M. Shen, Y. Su, R.-C. Hong, Y. Y. Lin, C.-C. Jeng, M.-F. Shih, and R.-K. Lee, "Observation of phase boundaries in spontaneous optical pattern formation," Phys. Rev. A **91**, 023810 (2015)
10. D. R. Solli, G. Herink, B. Jalali, and C. Ropers, "Fluctuations and correlations in modulation instability," Nature Photon. **6**, 463 (2012).
11. A. M. Rubenchik, S. K. Turitsyn, and M. P. Fedoruk, "Modulation instability in high power laser amplifiers," Opt. Express **18**, 1380 (2010).
12. M. Droques, B. Barviau, A. Kudlinski, M. Taki, A. Boucon, T. Sylvestre, and A. Mussot, "Symmetry-breaking dynamics of the modulational instability spectrum," Opt. Lett. **36**, 1359 (2011).
13. K. Nithyanandan, R. Vasantha Jayakantha Raja, and K. Porsezian "Modulational instability in a twin-core fiber with the effect of saturable nonlinear response and coupling coefficient dispersion," Phys. Rev. A **87**, 043805 (2013).
14. D. Kip, M. Soljacic, M. Segev, E. Eugenieva, and D. N. Christodoulides, "Modulation instability and pattern formation in spatially incoherent light beams," Science **290**, 495 (2000).
15. M. Soljacic, M. Segev, T. H. Coskun, D. N. Christodoulides, and A. Vishwanath, "Modulation instability of incoherent beams in noninstantaneous nonlinear media," Phys. Rev. Lett. **84**, 467 (2000).

#234867 - $15.00 USD Received 17 Feb 2015; revised 3 Apr 2015; accepted 3 Apr 2015; published 13 Apr 2015

16. M. F. Shih, C. C. Jeng, F. W. Sheu, and C. Y. Lin,"Spatiotemporal Optical Modulation Instability of Coherent Light in Noninstantaneous Nonlinear Media," Phys. Rev. Lett. **88**, 133902 (2002).
17. D. V. Dylov and J. W. Fleischer, "Modulation instability of a coherent-incoherent mixture," Opt. Lett. **35**, 2149 (2010).
18. W. Krolikowski, O. Bang, J. J. Rasmussen, and J. Wyller, "Modulational instability in nonlocal nonlinear Kerr media," Phys. Rev. E **64**, 016612 (2001).
19. A. Armaroli and F. Biancalana, "Tunable modulational instability sidebands via parametric resonance in periodically tapered optical fibers," Opt. Express **20**, 25096 (2012).
20. N.V. Kuktharev, V.B. Markov, S.G. Odulov, M.S. Soskin and L. Vinetskii, "Holographic storage in electrooptic crystals I," Ferroelectrics **22**, 949 (1979).
21. D. N. Christodoulides and M. I. Carvalho,"Bright, dark, and gray spatial soliton states in photorefractive media," J. Opt. Soc. Am. B **12**, 9 (1995).
22. C. Denz, M. Schwab, and C. Weilnau, *Transverse-Pattern Formation in Photorefractive Optics*, (Springer-Verlag, 2003).

Modulation instability (MI) is a universal signature of symmetry-breaking phenomena, which is driven through the stochastic fluctuations in nonlinear processes [1]. In different areas of nonlinear systems, such as sand ripples, cloud formations, water waves, and animal pigmentation, MI has been studied as a simple means to observe the manifestation of strongly nonlinear effects in nature [2–4]. In optics, it is MI that a small perturbation in the amplitude or phase could cause the input waves to grow exponentially, resulting in chaotic, solitary, and turbulence waves [5, 6]. Even though MI had been reported with biased photorefractive crystals a decade ago [7], until recently the existence of optical pattern transitions from MI in the uniform background to transverse instability in quasi two-dimensional structure is demonstred [8, 9].

Even though it is believed that MI is an intrinsic property in nonlinear systems, its role for the pattern competition and correlation in confined systems is revealed only through single-shot spectra produced by laser pulses [10]. Nevertheless, with higher-order dispersion, saturation of nonlinearity, and cross-talk among different channels, MI is accounted for one of the main factors responsible for the degradation of beam quality in high power laser systems [11–13]. Suppression or modification of MI is achieved by partial coherent light [14–17], nonlocal nonlinear media [18], or periodically tapered photonic crystal fibers [19].

In this work, we demonstrate the control of MI in photorefractive crystals experimentally and theoretically, by varying the ratio of background to signal intensities. Through a series of spontaneous optical patterns, appearance, suppression, and disappearance of MI images are demonstrated when the intensity of input coherent beam increases. Experimental measurements are also performed for different bias voltages. Based on the band transport model for photorefractive crystals, the dependence on the growth rate for perturbed modulated waves is shown as a function of the normalized signal intensity, which gives good agreement to the experimental measurements. The results in this work provide the possibility, not only in optics but also other areas of physics, to stabilize MI and related spontaneous symmetry-breaking instabilities.

In our experiment, as shown in Fig. 1, a continuous wave Nd:YVO4 diode-pumped solid state laser operated at double frequency, with the center wavelength at 532nm, is split into two polarized beams through a polarization beam splitter (PBS), as a control for the intensity ratio between two polarized beams. Then, the extraordinarily (signal) and ordinarily (background) polarized beams are collimated into the photorefractive medium, *i.e.*, a strontium-barium niobate (SBN:60) crystal. By applying a DC biased voltage on the crystal along the *c*-axis, spaced-charged field will be induced due to the electro-optical (Pockel) effect, which provides the required nonlinearity in our system. The SBN:60 crystal is 5mm in length and 5mm in thickness, which has an effective electro-optical coefficient about $r_{33} \approx 350$pm/V. With a charge-coupled device (CCD) camera, a series of self-organized optical patterns at the output plane is recorded as the signal light intensity varies. Detail experimental setup for the measurement of optical pattern transitions can be found in our previous work [8].

#234867 - $15.00 USD Received 17 Feb 2015; revised 3 Apr 2015; accepted 3 Apr 2015; published 13 Apr 2015

First of all, we fix the intensity ratio of background to signal beams at zero, *i.e.*, $r_{BS} \equiv I_B/I = 0$, but change the intensity of input beam for different bias voltages. Here the intensities of background and signal beams are denoted by I_B and I, respectively. By normalizing the signal intensity with respect to the thermal intensity I_{th}, a series of spontaneous optical patterns form when the normalized signal intensity I/I_{th} increases, as shown in the Upper-panel of Fig. 2. For example, we fixed the bias voltage $V = 0.35$kV. Below a certain threshold intensity, perturbations on top of a uniform input remain as small fluctuations as shown in Fig. 2(a); while above the threshold intensity, the perturbations grow rapidly and a uniform signal will breakup into stripes, as shown in Fig. 2(b). Here, the period of stripes in the measured images, $\approx 38\mu$m, is defined by the modulated sinusoidal wave with a maximum growth rate. Such a stripe pattern becomes more clearly as the signal intensity increases further, as shown in Fig. 2(c). However, when the signal intensity increases above a certain value, the generated stripes become less distinct and eventually disappear, as shown in Fig. 2(d)-2(f). The same series of optical patterns can be also observed for different bias voltages, as shown in Fig. 2(g)-2(l) and Fig. 2(m)-2(r) for $V = 0.27$kV and 0.20kV, respectively. It is well known that appearance of spontaneous optical pattern formations can be explained by MI, nevertheless, suppression and even disappearance of MI patterns with a higher signal intensity are unexpected. Moreover, as the bias voltage is proportional to the nonlinear coefficient, the threshold intensities for the appearance of MI stripes, and the subsequent disappearance, become larger as the bias voltage goes smaller. To have a quantitative analysis, we perform a 2D Fourier transform of the experimental measurement, and extract the maximum value in the magnitude as the modulation instability growth rate.

To illustrate the MI patterns, we follow the band transport model to describe charge transport mechanism in photorefractive crystals [20–22]. The generalized nonlinear Schrödinger equation is used for signal beams:

$$iA_z + \frac{1}{2}A_{xx} - \frac{\gamma(V)}{2}\int_{-\infty}^{t} F(|A(t')|^2)\frac{e^{-(t'-t)/\tau}}{\tau}\,dt'A = 0, \tag{1}$$

where $A(z,x,t') = \sqrt{I/I_{th}}$ is the slowly varying envelope of signal field, which is normalized with respected to the thermal intensity I_{th}. The nonlinear coefficient $\gamma(V) \propto r_{33}V$ is assumed

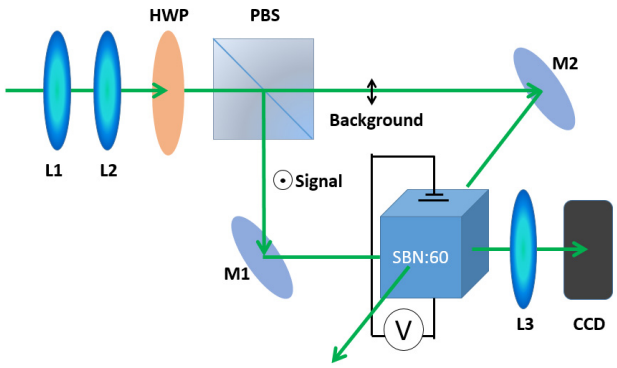

Fig. 1. Illustration of our experimental setup, where PBS is the polarization beam splitter, SBN:60 is the photorefractive crystal, HWP is a half-wave plate, L1 and L2 are two planoconvex lenses used for beam collimation, M1 and M2 are two reflecting mirrors, and L3 is an imaging lens to collect pattern images into the CCD camera.

#234867 - $15.00 USD Received 17 Feb 2015; revised 3 Apr 2015; accepted 3 Apr 2015; published 13 Apr 2015

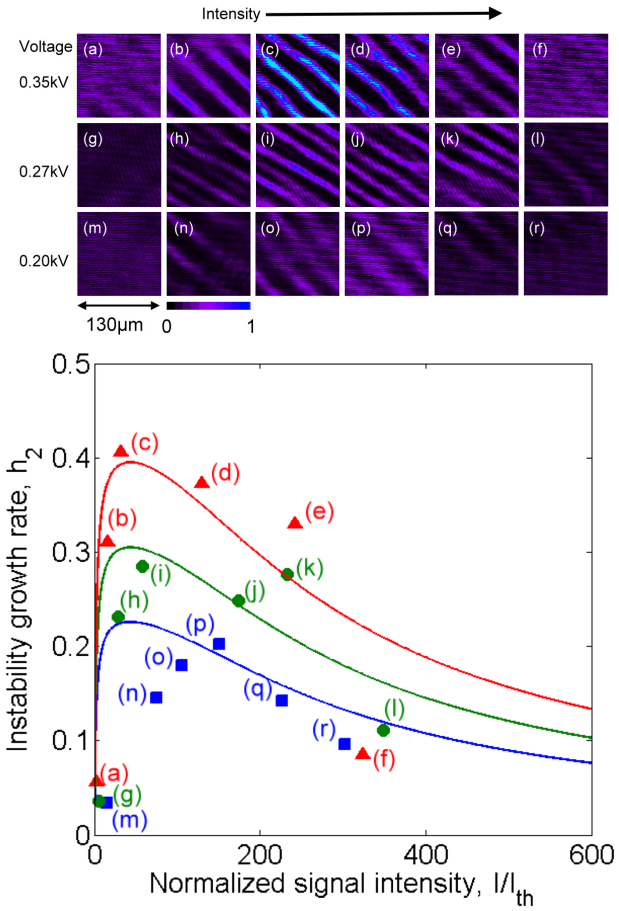

Fig. 2. Upper-panel: Optical intensity patterns of a coherent beam at the output plane through a nonlinear crystal at different bias voltages (shown in the left column) and different signal intensities (increase from left to right). Lower-panel: MI spectra for the instability growth rate h_2 versus the normalized signal intensity I/I_{th}. Theoretical curves for different bias voltages are depicted in solid-curves; while the labeled markers correspond to the experimental data shown in the Upper-panel. Here, the intensity ratio of background to signal beams is $r_{BS} = 0$.

linearly proportional to the bias voltage V. The nonlinear response function has the form:

$$F(|A|^2) = \frac{1}{1+(1+r_{BS})|A|^2}, \tag{2}$$

with r_{BS} denoting the ratio of background wave to signal wave intensities, which acts as the control parameter in this work. Due to the experimental condition used in Fig. 2, where $r_{BS} = 0$, it is noted that instead of normalization with respect to the background field, we keep the thermal intensity as the normalization unit, which is usually neglected. Moreover, without loss of generality, we also include a non-instantaneous response function with the delay time constant τ, which is inversely proportional to the signal intensity [16]

Then, by assuming the perturbation terms on top of a planewave solution, *i.e.*, $A = [A_0 + a_1(x,z,t) + i\,a_2(x,z,t)]\exp(-i\beta z)$, with $a_m = \mathrm{Re}[\varepsilon_m \exp(i\Omega t + i\,kx - i\,hz)]$ $(m = 1,2)$, the result

#234867 - $15.00 USD Received 17 Feb 2015; revised 3 Apr 2015; accepted 3 Apr 2015; published 13 Apr 2015

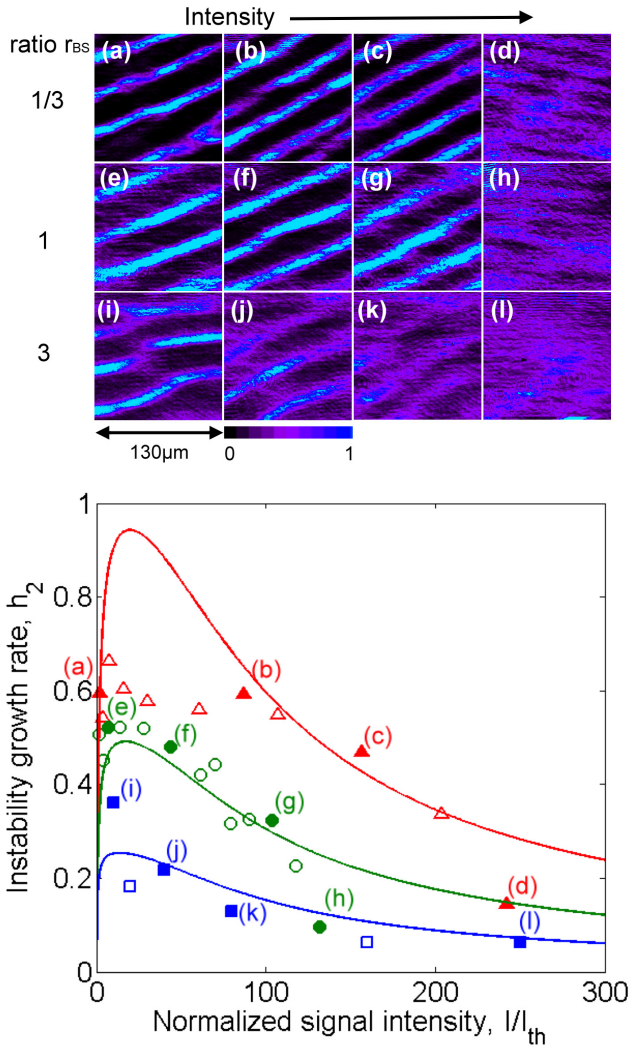

Fig. 3. Upper-panel: Optical intensity patterns measured at different intensity ratios (shown in the left column) and different signal intensities (increase from left to right). Lower-panel: MI spectra for the instability growth rate h_2 versus the normalized signal intensity I/I_{th}. Theoretical curves are depicted in solid-curves; while the labeled markers correspond to the experimental data shown in the Upper-panel. Here, unlabeled markers (with empty shapes) are additional measured data points not shown in the Upper-panel.

by linear stability analysis gives the corresponding growth rate $h_2 \equiv \mathrm{Im}[h]$:

$$h_2 = \pm \mathrm{Re}\left\{ \sqrt{\frac{\gamma}{2(1+i\Omega\tau)} \frac{(1+r_{BS})I}{[1+(1+r_{BS})I]^2} k^2 - \frac{k^4}{4}} \right\}, \tag{3}$$

with $I \equiv |A_0|^2$ being the normalized planewave intensity. When $\Omega\tau = 0$, our results apply for the instantaneous case.

In the Lower-panel of Fig. 2, we show the MI spectra based on Eq. (3) in the solid-curves with a constant background to signal ration $r_{BS} = 0$ for different bias voltages. Here, we choose

#234867 - $15.00 USD Received 17 Feb 2015; revised 3 Apr 2015; accepted 3 Apr 2015; published 13 Apr 2015

the thermal field intensity as $I_{th} = 0.7$, 1.56, and 2.8mW/cm^2 as a fitting parameter for the bias voltage at 0.2, 0.27, and 0.35kV, respectively. It can be seen that the instability growth rate h_2 grows first as a function of the normalized signal intensity, but decays as the signal intensity larger than a critical value, The instability growth rate reflects the appearance, suppression, and disappearance of MI patterns. A discrepancy between our experimental data and theoretical curve arises as the normalized signal intensity goes larger. With a larger signal intensity, higher-order nonlinearities induced through the interaction among space charges or a modified thermal field intensity may be the reason for such a discrepancy. However, compared to experimental images, shown by the markers, our theoretical curves not only give the tendency but also fit to the measured data, in particular in the low intensity region.

To further verify our control on the MI spectra, in Fig. 3, we perform another set of experiments by varying the intensity ratio of background to signal beams, *i.e.*, $r_{BS} = 1/3$, 1, and 3, respectively. Here, the corresponding biased voltages are fixed accordingly at slightly different values: 0.35, 0.4, and 0.8kV, respectively. As shown in the Upper-panel of Fig. 3, the measured images reveal the same scenario: first appearance, then suppression, and finally disappearance of stripe patterns as the normalized signal intensity increases. By plotting the instability growth rate versus the normalized signal intensity, we depict theoretical curves for different intensity ratio r_{BS} with experimental measured data in the Lower-panel of Fig. 3. Here, the fitting parameter for the thermal field intensity are chosen as $I_{th} = 7.3$, 4.3, and 1.0mW/cm^2 for the bias voltage at 0.35, 0.4, and 0.8kV, respectively. Again, a good agreement between theoretical model and experimental measurement is well demonstrated.

In summary, with experimental measurements and theoretical analyses, we demonstrate an alternative way to control optical pattern formations, particularly for the modulation instability in photorefractive crystals. By varying the ratio of background to input signal beam intensities, a series of spontaneous optical patterns is observed as the intensity of input coherent beam increases. Based on the band transport model, but keeping the thermal field, our theoretical results give a clear transition for the appearance, suppression, and disappearance of MI stripes. The results showed theoretically and experimentally here can also be useful for studying spatial-temporal pattern formations in higher dimensions for optical bullets, fluid dynamics, and plasma physics.

Acknowledgments

This work is supported in part by the Ministry of Science and Technologies, Taiwan, under the contract No. 101-2628-M-00 7-003-MY4 and No. 102-2212-M-005-002-MY3.

#234867 - $15.00 USD Received 17 Feb 2015; revised 3 Apr 2015; accepted 3 Apr 2015; published 13 Apr 2015